Nanotransducer-enabled deep-brain neuromodulation with NIR-II light

Xiang Wu[1,2], Fan Yang[1,2], Sa Cai[1,2], Kanyi Pu[3,4,*], and Guosong Hong[1,2,*]

[1] Department of Materials Science and Engineering, Stanford University, Stanford, CA, 94305, USA
[2] Wu Tsai Neurosciences Institute, Stanford University, Stanford, CA, 94305, USA
[3] School of Chemical and Biomedical Engineering, Nanyang Technological University, Singapore, Singapore
[4] Division of Chemistry and Biological Chemistry, School of Physical and Mathematical Sciences, Nanyang Technological University, Singapore, Singapore.
* Corresponding author: kypu@ntu.edu.sg; guosongh@stanford.edu

Abstract

The second near-infrared window (NIR-II window), which ranges from 1,000 to 1,700 nm in wavelength, exhibits unique advantages of reduced light scattering and thus deep penetration in biological tissues in comparison to the visible spectrum. The NIR-II window has been widely employed for deep-tissue fluorescence imaging in the past decade. More recently, deep-brain neuromodulation has been demonstrated in the NIR-II window by leveraging nanotransducers that can efficiently convert brain-penetrant NIR-II light into heat. In this Perspective, we discuss the principles and potential applications of this NIR-II deep-brain neuromodulation technique, together with its advantages and limitations compared with other existing optical methods for deep-brain neuromodulation. We also point out a few future directions where the advances in materials science and bioengineering can expand the capability and utility of NIR-II neuromodulation methods.

Main text

Neuromodulation techniques, capable of selectively activating or inhibiting certain subgroups of neurons, have a wide range of applications in both basic neuroscience research and therapeutic solutions.[1-3] Optogenetics, which uses light to control neural activities through microbial opsins,[4] has become a powerful tool in dissecting complex neural circuitries and even treating certain diseases in clinical trials.[2, 5] Conventional optogenetics uses visible light, which is strongly attenuated by the highly scattering brain tissue,[6, 7] thus necessitating chronic implantation of optical fibers for efficient light delivery in deep tissue.[8] Such invasive implantation is not ideal in both research and clinical settings, since it usually results in permanent neural tissue damage and physical tethering that restrains the head movement.[9, 10] Despite recent advances in novel *in vivo* neuromodulation techniques,[11-15] it remains challenging to optically modulate deep-brain neural activities in freely moving animals without any brain implant or head tethering.

The second near-infrared spectrum (NIR-II spectrum, 1,000-1,700 nm), compared to visible light, exhibits diminished scattering in biological tissues (especially the brain tissue) owing to the inversely proportional relationship of tissue scattering with wavelengths.[6, 16, 17] Therefore, NIR-II light represents a wireless means to interrogate and manipulate neural activity in the deep brain via properly designed nanotransducers. Specifically, photothermal nanotransducers, which efficiently convert light into heat, have been demonstrated to control neural activities through either temperature-sensitive ion channels or membrane capacitance change.[18-21] The wide

availability of nanomaterials that interact with light in the NIR-II window thus makes it possible to perform deep-brain neuromodulation in this advantageous spectrum.[22-24] Specifically, a nanotransducer-enabled NIR-II photothermal neuromodulation technique was recently reported to modulate deep-brain neural activities of freely moving mice in a tether-free and implant-free manner.[22, 25] Due to the exceptional photothermal performance of the nanotransducers and deep brain penetration of NIR-II light, this technique allowed behavioral studies of freely moving mice in a large arena and can potentially be applied for modulating neural activities in social interaction experiments.

In this perspective, we first provide a summary of existing optical methods for deep-brain neuromodulation, with an emphasis on their major advances and limitations. Afterwards, we discuss photothermal neuromodulation techniques based on different mechanisms. We then highlight the development and utilities of the recent NIR-II photothermal neuromodulation technique[22] and discuss how this new modality can resolve previously unaddressed challenges. In addition, we point out some limitations of this NIR-II photothermal neuromodulation approach at its current stage and present an outlook with a few potential directions in which this new modality can be further improved for enhanced capability and boarder applications. For a more comprehensive review of photothermal nanomaterials and nanotransducer-based neuromodulation techniques, we refer the readers to other existing reviews.[26-31]

Optical Methods for Deep-Brain Neuromodulation

Wireless Optogenetics. Since the demonstration of *in vivo* optogenetics neuromodulation using a fiber optics interface,[8] there have been many other optical approaches developed for deep-brain optogenetic neuromodulation (**Figure 1**).[11] One example is the wireless optogenetics approach using radio frequency (RF)-powered micro light emitting diode (μ-LED) devices (**Figure 1b**).[13, 32-34] Specifically, by leveraging recent advances in the fabrication and miniaturization of light emitting devices, Kim et al. demonstrated an injectable, cellular-scale μ-LED device that can be powered with RF scavenging.[13] One key advantage of this approach, compared with fiber-based optogenetics, lies in its wireless interface that frees the animal from physical tethering. Furthermore, the minimized footprint and reduced bending stiffness of the μ-LED device decreases the immune response at the neural interface compared to fiber optics. However, this method still requires a chronic implant inside the brain, which inevitably causes brain damage.

Upconversion nanoantenna. Another example is the upconversion nanoantenna-based optogenetics approach in the first near-infrared window (NIR-I window, 700-1000 nm) (**Figure 1c**).[14, 35, 36] Upconversion nanoparticles (UCNPs) exhibit the unique non-linear optical property of converting multiple longer-wavelength photons into one shorter-wavelength photon.[37] This property is particularly suitable for deep-brain applications, since NIR-I light experiences less scattering in the brain than visible light,[6] while many existing opsins only respond to short-wavelength visible light. Based on this advantage, Chen et al. demonstrated implant-free deep-brain optogenetics by stimulating intracranially delivered UCNPs with 980-nm illumination from a fiber fixed on the skull.[14] Yet, 980-nm is located near a major water absorption peak,[6] and the high power density used for deep-brain neuromodulation in this work induced a significant

temperature increase on the brain surface,[14] which may alter neural firings and even cause tissue damage.[38] Furthermore, head tethering from the skull-fixed fiber still requires scalp removal and imposes constraints on the animal's naturalistic behavior, while the intracranial delivery of UCNPs necessities invasive surgeries.

Red-shifted opsins. Furthermore, recent advances in protein engineering have resulted in red-shifted opsins with improved sensitivities.[12, 39] ChRmine, a potent channelrhodopsin, represents one of the most sensitive red-shifted opsins so far, with an effective power density for 50% activation (EPD50) of only 0.03 mW/mm^2 at 635 nm,[12] in contrast to 1.3 mW/mm^2 at 470 nm for the original channelrhodopsin-2 (ChR2).[40] Leveraging the ultra-high sensitivity of ChRmine, Chen et al. reported deep-brain neuromodulation with skull-fixed fiber optics up to a depth of 7-mm in rat brains (**Figure 1d**).[12] Combined with a systemic viral delivery approach that selectively transduced certain neuron subtypes,[41] ChRmine enabled surgery-free deep-brain optogenetics in mice. Notably, the illumination condition of 635 nm light used in this work only resulted in minimal heating on the brain surface. However, 635-nm light is still strongly scattered by the brain tissue,[6] necessitating light delivery through skull-fixed fibers, requiring scalp removal, and imposing physical tethering to the subject.

Sono-optogenetics. In addition, another non-invasive optogenetics approach, sono-optogenetics, was enabled by a circulation-delivered nanoscopic light sources (**Figure 1e**).[15, 42-45] Specifically, Wu et al. designed and synthesized ZnS-based mechanoluminescent nanoparticles (MLNPs) that can be activated by deep-penetrating focused ultrasound (FUS).[15] Upon systemic delivery, these MNLPs flow through the entire body, but only emit 470-nm light transiently at the ultrasound focus in the brain. Furthermore, the energy-depleted MNLPs can be recharged by an external excitation light source when they pass through superficial blood vessels. The use of an acoustic interface enables through-scalp optogenetics neuromodulation in live mice without any brain implants or scalp incision, but also necessitates close contact between the ultrasound transducer and the animal's head, since acoustic waves transmit poorly across the air-tissue interface. At the current stage, sono-optogenetics has only been demonstrated in head-fixed animals, but the development of wearable ultrasound transducers may enable sono-opotogenetics neuromodulation in freely moving subjects.[46-48]

Photothermal neuromodulation

It is desirable to modulate deep-brain neural activities in freely moving animals using a tether-free and implant-free interface, yet previous optical neuromodulation modalities cannot fulfill this requirement.[11] Specifically, for existing techniques that use light to penetrate through the overlying tissue and reach the target brain region, such as those based on upconversion nanoantennas (**Figure 1c**) and red-shifted opsins (**Figure 1d**),[12, 14] only far-red visible light or 980 nm light was used. These wavelengths are not ideal for deep-brain neuromodulation, since the scattering from the brain and the absorption from water and several bio-chromophores still remain significant.[6] In fact, the choice of excitation wavelengths for UCNPs is largely fixed by the intrinsic energy levels of lanthanide ions,[49] while that for red-shifted opsins is currently restricted to far-red visible light,[50] probably due to the difficulty of activating opsins with low-energy photons at longer wavelengths.

In contrast, photothermal nanomaterials offer a much wider range of wavelength selections, with many recent demonstrations of nanotransducers that respond to NIR-II light.[22-24] In this section, we first give a few examples of photothermal neuromodulations techniques based on different mechanisms, most of which were only demonstrated *in vitro*. We then present a discussion of a recently reported NIR-II photothermal deep-brain neuromodulation approach, and highlight how it can address previous challenges.

Activation of temperature-sensitive ion channels. One common mechanism for photothermal neuromodulation is through the activation of temperature-sensitive ion channels (**Figure 2**), such as TRP (transient receptor potential) channels. The activation of these channels results in the influx of cations across the cell membrane, thus depolarizing the cell. For example, Nakatsuji et al. used 785 nm light and gold nanorods (AuNRs) to activate cultured HEK293T cells that expressed temperature sensitive ion channel TRPV1 (TRP subfamily V member 1) (**Figure 2a**).[19] Furthermore, Lyu et al. demonstrated reproducible photothermal activation of TRPV1-expressing ND7/23 cells *in vitro* with 808 nm light and semiconducting polymer nanobioconjugates (SPNs), which showed better photothermal stability during multiple heating and cooling cycles than AuNRs (**Figure 2b**).[51] Additionally, Nelidova et al. recently adapted a similar strategy to stimulate mice retinal cones that expressed either rat TRPV1 or snake TRPA1 (TRP subfamily A member 1) (**Figure 2c**).[52] Specifically, they delivered AuNRs locally to the retina, and stimulated them with 915 nm or 980 nm NIR light. Using this strategy, they were able to restore vision in mice with retinal degeneration and evoke behavioral responses using visual cues.

Heat-induced membrane capacitance change. Another mechanism for photothermal neuromodulation is through membrane capacitance change induced by a transient and rapid temperature increase (**Figure 3**). The heat-induced membrane capacitance change then leads to a current flowing across the cell membrane to stimulate the cell. This mechanism was first proposed and validated by Shapiro et al., who used intense pulsed laser with wavelengths >1500 nm to rapidly heat up water and demonstrated cell stimulation in different biological systems, including oocytes, HEK cells and artificial neurons (**Figure 3a**).[20] Based on this mechanism, Carvalho-deSouza et al. used pulsed 532 nm light and surface-functionalized gold nanoparticles (AuNPs) to activate dorsal root ganglion (DRG) neurons *in vitro* and mice hippocampal neurons in acute brain slices (**Figure 3b**).[53] Furthermore, Jiang et al. designed biocompatible mesostructured silicon as the photothermal agent and used it to stimulate DRG neurons *in vitro* with pulsed 532 nm laser (**Figure 3c**).[18] Notably, the energy of a single laser pulse (5.32 μJ) used in this work was 30× lower than that in Ref. 53 that used AuNPs. Apart from extracellular interface with an entire cell, the same group also designed silicon nanowire as the photothermal agent for intracellular interface with organelles (**Figure 3d**).[54] Specifically, Jiang et al. used pulsed 592 nm light and internalized silicon nanowire to modulate glial activities *in vitro*, probably as a result of calcium release from internal organelles upon photothermal stimulation. More recently, Rastogi et al. designed fuzzy graphene consisting of 1D nanowires and 2D graphene flasks for photothermal neuromodulation in both 2D culture of DRG neurons and 3D culture of cortical spheroids using 405 nm or 635 nm light (**Figure 3e**).[55] Importantly, the high photothermal performance of fuzzy graphene allowed cell stimulation with an energy level of < 100 nJ per pulse, much lower than that in previous

works.[18, 53, 54] Similarly, Wang et al. recently used 2D $Ti_3C_2T_x$ MXene flakes for DRG neurons stimulation *in vitro* (**Figure 3f**).[56] Compared with fuzzy graphene, MXene flakes can also be effectively excited by 808 nm light, which is beneficial for future *in vivo* application due to the deeper penetration of NIR light.

Photothermal neural inhibition. Apart from neural activation, photothermal effects can also be utilized for neural inhibition (**Figure 4**). For example, Yoo et al. used AuNRs and 785 nm light to reversibly inhibit spontaneous activities of a neural network *in vitro* (**Figure 4a**).[57] They attributed the photothermal inhibition effect to temperature sensitive potassium channel TREK-1. More recently, Owen et al. showed that the illumination conditions commonly used for *in vivo* optogenetics neuromodulation may produce a significant thermal effect and inhibit activities of medium spiny neurons (MSNs) in the striatum of the mouse brain (**Figure 4b**).[38] Similarly, they also attributed this photothermal neural inhibition effect to the activation of an inwardly rectifying potassium channel (K_{ir}), the conductance of which depends on temperature.

NIR-II Photothermal Deep-Brain Neuromodulation. As summarized above, most of existing photothermal neuromodulation modalities were only demonstrated *in vitro*, with a stimulation wavelength in the visible or NIR-I region. Extending the photothermal neuromodulation toolbox to the NIR-II window is beneficial for *in vivo* applications due to the deeper penetration depth. Yet, going too far into the infrared spectrum is not desired, since water absorption becomes too significant beyond ca. 1500 nm.[58] Therefore, Wu et al. estimated the combined effect of scattering and absorption of brain tissue by plotting its effective attenuation coefficient in the entire 400-1800 nm spectrum.[22] The effective attenuation coefficient is defined as $\mu_{eff} = \sqrt{3\mu_a \cdot (\mu_a + \mu_s')}$,[59] where μ_a and μ_s' are the absorption coefficient and reduced scattering coefficient, respectively. As revealed in **Figure 5a**, the global minimum for light attenuation in the brain sits between 1050 and 1150 nm (effective attenuation coefficient ~ 0.28 mm^{-1}), and the choice of 1064-nm naturally stands out due to its wide availability enabled by Nd:YAG lasers. Inspired by this finding, the authors designed nanotransducers named MINDS (*m*acromolecular *i*nfrared *n*anotransducers for *d*eep-brain *s*timulation), which exhibit strong absorption at 1064-nm as a result of rational tuning of the highest occupied and lowest unoccupied molecular orbitals (**Figure 5b,c**). Specifically, the 40-nm MINDS consist of a NIR-II absorbing core of pBBTV (poly(benzobisthiadiazole-alt-vinylene) with a photothermal conversion efficiency of 71%, and an FDA-approved amphiphilic shell of PLGA-PEG (poly(lactide-co-glycolide)-b-poly(ethylene glycol)) to improve biocompatibility (**Figure 5b**). The molar absorption coefficient and mass-normalized absorption coefficient of MINDS are 5.52×10^9 M^{-1} cm^{-1} and 23.6 L g^{-1} cm^{-1}, respectively. Due to the strong absorption at 1064 nm and superior photothermal performance of MINDS, through-scalp wide-field 1064-nm illumination created a local hot spot around MINDS injected in the deep brain, while only inducing a negligible temperature increase at the brain surface (**Figure 5d**). This differential heating capability is essential for NIR-II neuromodulation by exposing the animal to irradiation within the safety limit.[60] The authors also confirmed that the illumination conditions used in this study would not result in thermal damage or ablation effect in the brain tissue.[22]

The heat generated by MINDS under NIR-II illumination was transferred to ectopically expressed TRPV1 channels for neural activation (**Figure 1f**).[22] To demonstrate the *in vivo* utility of this bioinspired NIR-II neuromodulation technique, Wu et al. selectively transduced TRPV1 into dopaminergic neurons in the ventral tegmental area (VTA), which is a hub of the reward circuitry in the mouse brain,[61] and injected the MINDS solution to the same region (**Figure 5e**).[22] They studied the neuromodulation effect via a conditioned place preference test in a Y-maze.[13, 61] Specifically, mice were allowed to explore the entire arena freely, while NIR-II illumination was confined in one of the arm terminals with a specific wall pattern (**Figure 5f**).[22] Notably, the source of NIR-II illumination was placed ~1 m above the mouse head, leaving no device in the proximity of the freely moving subject. After 3 days of conditioning with NIR-II illumination, the animals exhibited a strong place preference for the arm terminal with NIR-II illumination, while control mice lacking either TRPV1, MINDS, or both did not show any place preference (**Figure 5g**).[22] These results confirm successful deep-brain neuromodulation of dopaminergic neurons with NIR-II light.

Compared with other existing optical deep-brain neuromodulation modalities discussed above, this recent demonstration of NIR-II neuromodulation enables remote neural stimulation of freely moving animals via an implant-free and tether-free interface.[22] Therefore, brain-penetrant NIR-II illumination enables neuromodulation in animal behavioral experiments without perturbing the naturalistic behaviors of the subject, thus enabling potential applications for manipulating the neural activities of socially interacting animals.

Outlook and Future Directions

Although this new NIR-II neuromodulation approach overcomes some challenges in previous methods, at the current stage it still has a few limitations that warrant further improvements. In this section, we present discussions about these limitations and include an outlook for each limitation on how advances in materials science and bioengineering can push the boundaries of NIR-II neuromodulation strategies (**Figure 6**).

Faster response times. The response time for the current NIR-II neuromodulation technique is ~ 1 s *in vitro* and a few seconds for *in vivo* behavioral experiments, as a result of the threshold activation behavior of TRPV1.[22] Although this second-level time delay is much faster than those for chemogenetics or magnetothermal neuromodulation in rodents,[62-65] it is still longer than the millisecond-level response time for most optogenetics approaches, which makes this technique unsuitable to study fast neural dynamics.[4] Furthermore, this second-level response time leads to a thermal diffusion length on the scale of millimeter, thus placing a large volume of brain tissue at the risk of thermal damage. Note that the power density used for NIR-II deep-brain neuromodulation (10 mW/mm^2) is already approaching the maximum permissible exposure at 1064 nm,[60] thus disallowing a faster response time by simply increasing the laser power. One straightforward way of shortening this response time is to design new materials with higher absorption and more efficient photothermal energy conversion. However, considering the photothermal conversion efficiency of MINDS is already close to unity (71%),[22] pushing the

nanotransducer to the physical limit of its photothermal efficiency may not result in a significant improvement on the response time.

Recently, Sebasta et al. demonstrated sub-second magnetothermal neural activation in fruit flies using a temperature rate-sensitive ion channel *Drosophila* TRPA1-A (dTRPA1-A).[66] In contrast to TRPV1, which has a fixed activation temperature,[67] the activation threshold of dTRPA1-A decreases at a high temperature increase rate,[68] thus allowing fast magnetothermal neuromodulation during rapid heating with a small absolute temperature change.[66] However, dTRPA1-A cannot be directly applied to mammals, since its activation threshold is lower than 37 ^{o}C and will thus be constantly activated at body temperature.[66] Nonetheless, this recent demonstration suggests that other engineered or naturally originating rate-sensitive ion channels with their activation thresholds slightly higher than the mammalian body temperature can potentially enable fast photothermal neuromodulation in rodents (**Figure 6a**). Furthermore, the resulting shorter latency time and lower absolute temperature increases will also significantly reduce the potential risk of thermal damage in the brain tissue.

Multiplexing. In the current NIR-II neuromodulation method, the authors only demonstrated neural activation with a single wavelength of NIR-II light.[22] Therefore, a potential improvement lies in the ability of multiplexed stimulation with different illumination wavelengths. Multiplexing has the benefit of probing different populations of neurons inside the same subject simply by altering the wavelength parameter of the light stimulus. Recently, multichannel magnetothermal neural stimulation has been achieved using different nanomaterials that heat up under sufficiently different field strengths and frequencies of alternating magnetic fields.[66, 69] A similar idea can be leveraged to achieve multiplexing in photothermal neuromodulation using nanotransducers with sufficiently different absorption peaks. However, since there is only a narrow spectral window that allows deep tissue penetration (**Figure 5a**),[22] it is essential to design nanotransducers with very sharp absorption peaks to avoid any crosstalk between neighboring channels (**Figure 6b**). In this respect, AuNRs can be promising candidates for achieving multiplexing due to their narrow bandwidth and wide wavelength tunability.[70, 71] However, even the absorption peaks of AuNRs are too wide to achieve multiplexing within the narrow range of 1050-1100 nm, and a compromising solution would be to move one absorption peak to the secondary local minimum in the range of 700-900 nm (effective attenuation coefficient ~ 0.33 mm^{-1} at 800 nm, **Figure 5a**). Apart from AuNRs, a recent demonstration of silica-coated semiconductor microcavities affording whispery gallery modes might be leveraged to design photothermal systems with extremely narrow bandwidth,[72] thus allowing fitting two or more photothermal channels in the 1050-1100 nm range.

Non-genetic NIR-II deep-brain neuromodulation. Another limitation for the current NIR-II neuromodulation method lies in the need for genetic modification. Although the selective expression of TRPV1 enables cell-type specific neuromodulation, it also presents an obstacle for potential clinical translation. Recently, Zhang et al. demonstrated non-genetic NIR-II photothermal neuromodulation in behaving mice with bioinspired nano-vesicles,[73] which convert short but intense NIR-II pules into rapid temperature increases that modulate neural activities through the membrane capacitance change.[20] Nonetheless, only neuromodulation in the motor

cortex and hippocampus was demonstrated with a fiber fixed on the scalp, while the feasibility of remote NIR-II neuromodulation in deeper brain regions remains to be explored. Besides, the acoustic wave generated by the photothermal effect has also been utilized for non-genetic neuromodulation *in vivo*.[74, 75] Specifically, Jiang et al. designed semiconducting polymer nanoparticles that generate photoacoustic waves upon nanosecond NIR-II pulses, which activated endogenously expressed mechanosensitive ion channel TRPV4 and modulated neural activities in the primary motor cortex in mice.[75] However, this NIR-II photoacoustic neuromodulation technique requires fiber implantation for efficient light delivery at its current stage. Nonetheless, further optimization of current photothermal nanomaterials with extremely high absorption may enable tether-free and implant-free NIR-II neuromodulation in the deep brain via either the membrane capacitance change or the acoustic activation mechanism in the future (**Figure 6c**).

As the light pulse duration in these two methods is on the level of millisecond to nanosecond, it is important to optimize the thermal conductance of the coating layer on the nanotransducer surface to enable fast thermal diffusion from the nanotransducers to the cell membrane or receptors of interest. Furthermore, since both mechanisms require rapid temperature changes and thus intense NIR-II pulses, one potential concern arises from the transient temperature increase in the superficial tissue that may lead to thermal damage therein. Thus, appropriate controls and thermal damage assessment should always be included to rule out confounding factors and confirm the safety of NIR-II exposure protocols. Besides, other non-thermal neuromodulation mechanisms, such as photovoltaic neural stimulation and azobenzene-based photoswitches,[76-79] may also be leveraged to achieve non-genetic deep-brain neuromodulation if the corresponding material toolbox can be extended to the NIR-II region with sufficient efficiency.

Surgery-free NIR-II neuromodulation. Although NIR-II light can penetrate deep into the brain and modulate neural activities in a non-invasive manner, the deliveries of MINDS and adeno-associated virus (AAV) encoding TRPV1 still require invasive intracranial surgeries. To mitigate this remaining level of invasiveness, systemic delivery methods for MINDS and TRPV1 can be adapted (**Figure 6d**). For example, ultrasound-mediated blood-brain-barrier (BBB) opening may be leveraged for non-invasive deliveries of both MINDS and TRPV1.[80, 81] Specifically, the development of an ultrasound responsive liposome system that can simultaneously deliver both MINDS and AAV in a single intravenous injection and ultrasound session will greatly simplify the procedure and reduce the perturbation to the animal.[82] Furthermore, systemic delivery of TRPV1 to target a specific type of neurons inside the brain can also be achieved by leveraging the recently developed AAV-PHP.eB virus.[41]

Final remarks. Functional nanotransducers have been exploited to enable novel neural interfaces,[27] with a recent demonstration of NIR-II deep-brain neuromodulation in freely moving animals based on photothermal nanotransducers.[22] Compared with existing optical deep-brain neuromodulation approaches, this NIR-II neuromodulation method eliminates any brain implant or head tethering, thus allowing remote neural activation in freely moving animals (**Figure 1**). However, this method at its current stage still has some limitations, such as the second-level response time, the lack of multiplexing, the need for genetic modification, and the remaining

invasiveness associated with intracranial surgeries. Nonetheless, with the rapid expansion of functional biomaterials and bioengineering toolboxes, these limitations of NIR-II neuromodulation will be mitigated in the near future (**Figure 6**). Furthermore, apart from neuromodulation, infrared photothermal systems based on nanotransducers have also been used in other emerging fields in biology, such as CRISPR-Cas9-mediated genome modifications and chimeric antigen receptor (CAR) T-cell therapies.[83, 84] Thus, we envision that with further optimization and development, NIR-II photothermal system will eventually become a versatile platform for studying and controlling various biological processes.

Although NIR-II light can penetrate through the entire mouse brain (~6 mm in depth), it remains challenging to reach the deep regions in the human brain (>10 cm in depth). Such limitation comes from the intrinsic light-tissue interaction, with one potential direction to address this challenge by looking at other frequency ranges in the electromagnetic spectrum for much deeper penetration. For example, radiofrequency waves such as WiFi can penetrate tens of centimeters in biological tissues, and we thus envision that the development of biomaterials which can strongly interact with RF signals may eventually enable noninvasive neuromodulation throughout the entire human brain.[85-87]

Acknowledgement
X.W. acknowledges support from the Stanford Graduate Fellowship. S. C. acknowledges support from the Stanford Bio-X Graduate Fellowship and the NeuroTech training program supported by the National Science Foundation under Grant No. 1828993. K.P. thanks Nanyang Technological University (startup grant: M4081627) and Singapore Ministry of Education Academic Research Fund Tier 2 (MOE2016-T2-1-098) for financial support. G.H. acknowledges startup support from the Wu Tsai Neurosciences Institute of Stanford University, a National Institutes of Health (NIH) Pathway to Independence Award (National Institute on Aging 5R00AG056636-04), a National Science Foundation (NSF) CAREER Award (2045120), the Rita Allen Foundation Scholars Program, a gift from the Spinal Muscular Atrophy (SMA) Foundation, and seed grants from the Wu Tsai Neurosciences Institute and the Bio-X Initiative of Stanford University. Some schematics were created with BioRender.com.

Author Contributions
The manuscript was written through contributions of all authors. All authors have given approval to the final version of the manuscript.

Notes
The authors declare no conflicts of interest.

References
1. Lozano, A. M.; Lipsman, N.; Bergman, H.; Brown, P.; Chabardes, S.; Chang, J. W.; Matthews, K.; McIntyre, C. C.; Schlaepfer, T. E.; Schulder, M.; Temel, Y.; Volkmann, J.; Krauss, J. K., Deep brain stimulation: current challenges and future directions. *Nat. Rev. Neurol.* **2019,** *15* (3), 148-160.

2. Fenno, L.; Yizhar, O.; Deisseroth, K., The development and application of optogenetics. *Annu. Rev. Neurosci.* **2011,** *34*, 389-412.
3. Chen, R.; Canales, A.; Anikeeva, P., Neural Recording and Modulation Technologies. *Nat. Rev. Mater.* **2017,** *2* (2), 16093.
4. Boyden, E. S.; Zhang, F.; Bamberg, E.; Nagel, G.; Deisseroth, K., Millisecond-timescale, genetically targeted optical control of neural activity. *Nat. Neurosci.* **2005,** *8* (9), 1263-1268.
5. Sahel, J. A.; Boulanger-Scemama, E.; Pagot, C.; Arleo, A.; Galluppi, F.; Martel, J. N.; Esposti, S. D.; Delaux, A.; de Saint Aubert, J. B.; de Montleau, C.; Gutman, E.; Audo, I.; Duebel, J.; Picaud, S.; Dalkara, D.; Blouin, L.; Taiel, M.; Roska, B., Partial recovery of visual function in a blind patient after optogenetic therapy. *Nat. Med.* **2021,** *27* (7), 1223-1229.
6. Hong, G.; Antaris, A. L.; Dai, H., Near-infrared fluorophores for biomedical imaging. *Nat. Biomed. Eng.* **2017,** *1*, 0010.
7. Yaroslavsky, A. N.; Schulze, P. C.; Yaroslavsky, I. V.; Schober, R.; Ulrich, F.; Schwarzmaier, H. J., Optical properties of selected native and coagulated human brain tissues in vitro in the visible and near infrared spectral range. *Phys. Med. Biol.* **2002,** *47* (12), 2059-2073.
8. Zhang, F.; Gradinaru, V.; Adamantidis, A. R.; Durand, R.; Airan, R. D.; de Lecea, L.; Deisseroth, K., Optogenetic interrogation of neural circuits: technology for probing mammalian brain structures. *Nat. Protoc.* **2010,** *5* (3), 439-456.
9. Chen, Y.; Rommelfanger, N. J.; Mahdi, A. I.; Wu, X.; Keene, S. T.; Obaid, A.; Salleo, A.; Wang, H.; Hong, G., How is flexible electronics advancing neuroscience research? *Biomaterials* **2021,** *268*, 120559.
10. Salatino, J. W.; Ludwig, K. A.; Kozai, T. D. Y.; Purcell, E. K., Glial responses to implanted electrodes in the brain. *Nat. Biomed. Eng.* **2017,** *1* (11), 862-877.
11. Jiang, S.; Wu, X.; Rommelfanger, N. J.; Ou, Z. H.; Hong, G. S., Shedding light on neurons: optical approaches for neuromodulation. *Natl. Sci. Rev.* **2022,** *9*, nwac007.
12. Chen, R.; Gore, F.; Nguyen, Q. A.; Ramakrishnan, C.; Patel, S.; Kim, S. H.; Raffiee, M.; Kim, Y. S.; Hsueh, B.; Krook-Magnusson, E.; Soltesz, I.; Deisseroth, K., Deep brain optogenetics without intracranial surgery. *Nat. Biotechnol.* **2021,** *39* (2), 161-164.
13. Kim, T.-i.; McCall, J. G.; Jung, Y. H.; Huang, X.; Siuda, E. R.; Li, Y.; Song, J.; Song, Y. M.; Pao, H. A.; Kim, R.-H.; Lu, C.; Lee, S. D.; Song, I.-S.; Shin, G.; Al-Hasani, R.; Kim, S.; Tan, M. P.; Huang, Y.; Omenetto, F. G.; Rogers, J. A.; Bruchas, M. R., Injectable, Cellular-Scale Optoelectronics with Applications for Wireless Optogenetics. *Science* **2013,** *340* (6129), 211-216.
14. Chen, S.; Weitemier, A. Z.; Zeng, X.; He, L.; Wang, X.; Tao, Y.; Huang, A. J. Y.; Hashimotodani, Y.; Kano, M.; Iwasaki, H.; Parajuli, L. K.; Okabe, S.; Teh, D. B. L.; All, A. H.; Tsutsui-Kimura, I.; Tanaka, K. F.; Liu, X.; McHugh, T. J., Near-infrared deep brain stimulation via upconversion nanoparticle-mediated optogenetics. *Science* **2018,** *359* (6376), 679-684.
15. Wu, X.; Zhu, X.; Chong, P.; Liu, J.; Andre, L. N.; Ong, K. S.; Brinson, K., Jr.; Mahdi, A. I.; Li, J.; Fenno, L. E.; Wang, H.; Hong, G., Sono-optogenetics facilitated by a circulation-delivered rechargeable light source for minimally invasive optogenetics. *Proc. Natl. Acad. Sci. USA* **2019,** *116* (52), 26332-26342.
16. Kenry; Duan, Y.; Liu, B., Recent Advances of Optical Imaging in the Second Near-Infrared Window. *Adv. Mater.* **2018,** *30* (47), e1802394.
17. Hong, G.; Diao, S.; Chang, J.; Antaris, A. L.; Chen, C.; Zhang, B.; Zhao, S.; Atochin, D. N.; Huang, P. L.; Andreasson, K. I.; Kuo, C. J.; Dai, H., Through-skull fluorescence imaging of the brain in a new near-infrared window. *Nat. Photonics* **2014,** *8* (9), 723-730.

18. Jiang, Y.; Carvalho-de-Souza, J. L.; Wong, R. C.; Luo, Z.; Isheim, D.; Zuo, X.; Nicholls, A. W.; Jung, I. W.; Yue, J.; Liu, D. J.; Wang, Y.; De Andrade, V.; Xiao, X.; Navrazhnykh, L.; Weiss, D. E.; Wu, X.; Seidman, D. N.; Bezanilla, F.; Tian, B., Heterogeneous silicon mesostructures for lipid-supported bioelectric interfaces. *Nat. Mater.* **2016,** *15* (9), 1023-1030.
19. Nakatsuji, H.; Numata, T.; Morone, N.; Kaneko, S.; Mori, Y.; Imahori, H.; Murakami, T., Thermosensitive Ion Channel Activation in Single Neuronal Cells by Using Surface-Engineered Plasmonic Nanoparticles. *Angew. Chem. Int. Ed.* **2015,** *54* (40), 11725-11729.
20. Shapiro, M. G.; Homma, K.; Villarreal, S.; Richter, C. P.; Bezanilla, F., Infrared light excites cells by changing their electrical capacitance. *Nat. Commun.* **2012,** *3*, 736.
21. de Boer, W.; Hirtz, J. J.; Capretti, A.; Gregorkiewicz, T.; Izquierdo-Serra, M.; Han, S.; Dupre, C.; Shymkiv, Y.; Yuste, R., Neuronal photoactivation through second-harmonic near-infrared absorption by gold nanoparticles. *Light. Sci. Appl.* **2018,** *7*, 100.
22. Wu, X.; Jiang, Y.; Rommelfanger, N. J.; Yang, F.; Zhou, Q.; Yin, R.; Liu, J.; Cai, S.; Ren, W.; Shin, A.; Ong, K. S.; Pu, K.; Hong, G., Tether-free photothermal deep-brain stimulation in freely behaving mice via wide-field illumination in the near-infrared-II window. *Nat. Biomed. Eng.* **2022,** *6* (6), 754-770.
23. Jiang, Y.; Huang, J.; Xu, C.; Pu, K., Activatable polymer nanoagonist for second near-infrared photothermal immunotherapy of cancer. *Nat. Commun.* **2021,** *12*, 742.
24. Jiang, Y.; Zhao, X.; Huang, J.; Li, J.; Upputuri, P. K.; Sun, H.; Han, X.; Pramanik, M.; Miao, Y.; Duan, H.; Pu, K.; Zhang, R., Transformable hybrid semiconducting polymer nanozyme for second near-infrared photothermal ferrotherapy. *Nat. Commun.* **2020,** *11*, 1857.
25. Wu, X.; Hong, G., Protocol for wireless deep brain stimulation in freely behaving mice with infrared light. *STAR Protoc.* **2022,** *4* (1), 101757.
26. Liu, Y.; Bhattarai, P.; Dai, Z.; Chen, X., Photothermal therapy and photoacoustic imaging via nanotheranostics in fighting cancer. *Chem. Soc. Rev.* **2019,** *48* (7), 2053-2108.
27. Yang, X.; McGlynn, E.; Das, R.; Pasca, S. P.; Cui, B.; Heidari, H., Nanotechnology Enables Novel Modalities for Neuromodulation. *Adv. Mater.* **2021,** *33* (52), e2103208.
28. Li, X.; Xiong, H.; Rommelfanger, N.; Xu, X.; Youn, J.; Slesinger, P. A.; Hong, G.; Qin, Z., Nanotransducers for Wireless Neuromodulation. *Matter* **2021,** *4* (5), 1484-1510.
29. Acaron Ledesma, H.; Li, X.; Carvalho-de-Souza, J. L.; Wei, W.; Bezanilla, F.; Tian, B., An atlas of nano-enabled neural interfaces. *Nat. Nanotechnol.* **2019,** *14* (7), 645-657.
30. Xu, C.; Pu, K., Second near-infrared photothermal materials for combinational nanotheranostics. *Chem. Soc. Rev.* **2021,** *50* (2), 1111-1137.
31. Wang, Y.; Garg, R.; Cohen-Karni, D.; Cohen-Karni, T., Neural modulation with photothermally active nanomaterials. *Nat. Rev. Bioeng.* **2023**.
32. Montgomery, K. L.; Yeh, A. J.; Ho, J. S.; Tsao, V.; Mohan Iyer, S.; Grosenick, L.; Ferenczi, E. A.; Tanabe, Y.; Deisseroth, K.; Delp, S. L.; Poon, A. S., Wirelessly powered, fully internal optogenetics for brain, spinal and peripheral circuits in mice. *Nat. Methods* **2015,** *12* (10), 969-974.
33. Park, S. I.; Brenner, D. S.; Shin, G.; Morgan, C. D.; Copits, B. A.; Chung, H. U.; Pullen, M. Y.; Noh, K. N.; Davidson, S.; Oh, S. J.; Yoon, J.; Jang, K. I.; Samineni, V. K.; Norman, M.; Grajales-Reyes, J. G.; Vogt, S. K.; Sundaram, S. S.; Wilson, K. M.; Ha, J. S.; Xu, R.; Pan, T.; Kim, T. I.; Huang, Y.; Montana, M. C.; Golden, J. P.; Bruchas, M. R.; Gereau, R. W. t.; Rogers, J. A., Soft, stretchable, fully implantable miniaturized optoelectronic systems for wireless optogenetics. *Nat. Biotechnol.* **2015,** *33* (12), 1280-1286.

34. Yang, Y.; Wu, M.; Vazquez-Guardado, A.; Wegener, A. J.; Grajales-Reyes, J. G.; Deng, Y.; Wang, T.; Avila, R.; Moreno, J. A.; Minkowicz, S.; Dumrongprechachan, V.; Lee, J.; Zhang, S.; Legaria, A. A.; Ma, Y.; Mehta, S.; Franklin, D.; Hartman, L.; Bai, W.; Han, M.; Zhao, H.; Lu, W.; Yu, Y.; Sheng, X.; Banks, A.; Yu, X.; Donaldson, Z. R.; Gereau, R. W. t.; Good, C. H.; Xie, Z.; Huang, Y.; Kozorovitskiy, Y.; Rogers, J. A., Wireless multilateral devices for optogenetic studies of individual and social behaviors. *Nat. Neurosci.* **2021,** *24* (7), 1035-1045.
35. Wang, Y.; Lin, X.; Chen, X.; Xu, Z.; Zhang, W.; Liao, Q.; Duan, X.; Wang, X.; Liu, M.; Wang, F.; He, J.; Shi, P., Tetherless near-infrared control of brain activity in behaving animals using fully implantable upconversion microdevices. *Biomaterials* **2017,** *142*, 136-148.
36. Miyazaki, T.; Chowdhury, S.; Yamashita, T.; Matsubara, T.; Yawo, H.; Yuasa, H.; Yamanaka, A., Large Timescale Interrogation of Neuronal Function by Fiberless Optogenetics Using Lanthanide Micro-particles. *Cell Rep.* **2019,** *26* (4), 1033-1043.
37. Zhou, J.; Liu, Q.; Feng, W.; Sun, Y.; Li, F., Upconversion luminescent materials: advances and applications. *Chem. Rev.* **2015,** *115* (1), 395-465.
38. Owen, S. F.; Liu, M. H.; Kreitzer, A. C., Thermal constraints on in vivo optogenetic manipulations. *Nat. Neurosci.* **2019,** *22* (7), 1061-1065.
39. Lin, J. Y.; Knutsen, P. M.; Muller, A.; Kleinfeld, D.; Tsien, R. Y., ReaChR: a red-shifted variant of channelrhodopsin enables deep transcranial optogenetic excitation. *Nat. Neurosci.* **2013,** *16* (10), 1499-1508.
40. Mattis, J.; Tye, K. M.; Ferenczi, E. A.; Ramakrishnan, C.; O'Shea, D. J.; Prakash, R.; Gunaydin, L. A.; Hyun, M.; Fenno, L. E.; Gradinaru, V.; Yizhar, O.; Deisseroth, K., Principles for applying optogenetic tools derived from direct comparative analysis of microbial opsins. *Nat. Methods* **2011,** *9* (2), 159-172.
41. Chan, K. Y.; Jang, M. J.; Yoo, B. B.; Greenbaum, A.; Ravi, N.; Wu, W. L.; Sanchez-Guardado, L.; Lois, C.; Mazmanian, S. K.; Deverman, B. E.; Gradinaru, V., Engineered AAVs for efficient noninvasive gene delivery to the central and peripheral nervous systems. *Nat. Neurosci.* **2017,** *20* (8), 1172-1179.
42. Yang, F.; Wu, X.; Cui, H.; Jiang, S.; Ou, Z.; Cai, S.; Hong, G., Palette of Rechargeable Mechanoluminescent Fluids Produced by a Biomineral-Inspired Suppressed Dissolution Approach. *J. Am. Chem. Soc.* **2022,** *144* (40), 18406-18418.
43. Yang, F.; Wu, X.; Cui, H.; Ou, Z.; Jiang, S.; Cai, S.; Zhou, Q.; Wong, B. G.; Huang, H.; Hong, G., A biomineral-inspired approach of synthesizing colloidal persistent phosphors as a multicolor, intravital light source. *Sci. Adv.* **2022,** *8* (30), eabo6743.
44. Yang, F.; Kim, S. J.; Wu, X.; Cui, H.; Hahn, S. K.; Hong, G., Principles and applications of sono-optogenetics. *Adv. Drug Deliv. Rev.* **2023,** *194*, 114711.
45. Wang, W.; Wu, X.; Kevin Tang, K. W.; Pyatnitskiy, I.; Taniguchi, R.; Lin, P.; Zhou, R.; Capocyan, S. L. C.; Hong, G.; Wang, H., Ultrasound-Triggered In Situ Photon Emission for Noninvasive Optogenetics. *J. Am. Chem. Soc.* **2023,** *145* (2), 1097-1107.
46. Xian, Q. Q., Z.; Kala, S.; Wong, K. F.; Murugappan, S.; Wu, Y.; Hou, X.; Zhu, J.; Guo, J.; Sun, L., Circuit-specific sonogenetic stimulation of the deep brain elicits distinct signaling and behaviors in freely moving mice. *bioRxiv* **2021**, https://doi.org/10.1101/2021.11.06.467579.
47. Wang, C.; Li, X.; Hu, H.; Zhang, L.; Huang, Z.; Lin, M.; Zhang, Z.; Yin, Z.; Huang, B.; Gong, H.; Bhaskaran, S.; Gu, Y.; Makihata, M.; Guo, Y.; Lei, Y.; Chen, Y.; Li, Y.; Zhang, T.; Chen, Z.; Pisano, A. P.; Zhou, Q.; Xu, S., Monitoring of the central blood pressure waveform via a conformal ultrasonic device. *Nat. Biomed. Eng.* **2018,** *2* (9), 687-695.

48. Xu, K. Y., Y.; Hu, Z.; Yue, Y.; Cui, J.; Culver, J. P.; Bruchas, M. R.; Chen, H., TRPV1-mediated sonogenetic neuromodulation of motor cortex in freely moving mice. *bioRxiv* **2022**, https://doi.org/10.1101/2022.10.28.514307.
49. Zheng, W.; Huang, P.; Tu, D.; Ma, E.; Zhu, H.; Chen, X., Lanthanide-doped upconversion nano-bioprobes: electronic structures, optical properties, and biodetection. *Chem. Soc. Rev.* **2015,** *44* (6), 1379-1415.
50. Baker, C. K.; Flannery, J. G., Innovative Optogenetic Strategies for Vision Restoration. *Front. Cell. Neurosci.* **2018,** *12*, 316.
51. Lyu, Y.; Xie, C.; Chechetka, S. A.; Miyako, E.; Pu, K., Semiconducting Polymer Nanobioconjugates for Targeted Photothermal Activation of Neurons. *J. Am. Chem. Soc.* **2016,** *138* (29), 9049-9052.
52. Nelidova, D.; Morikawa, R. K.; Cowan, C. S.; Raics, Z.; Goldblum, D.; Scholl, H. P. N.; Szikra, T.; Szabo, A.; Hillier, D.; Roska, B., Restoring light sensitivity using tunable near-infrared sensors. *Science* **2020,** *368* (6495), 1108-1113.
53. Carvalho-de-Souza, J. L.; Treger, J. S.; Dang, B.; Kent, S. B.; Pepperberg, D. R.; Bezanilla, F., Photosensitivity of neurons enabled by cell-targeted gold nanoparticles. *Neuron* **2015,** *86* (1), 207-217.
54. Jiang, Y.; Li, X.; Liu, B.; Yi, J.; Fang, Y.; Shi, F.; Gao, X.; Sudzilovsky, E.; Parameswaran, R.; Koehler, K.; Nair, V.; Yue, J.; Guo, K.; Tsai, H. M.; Freyermuth, G.; Wong, R. C. S.; Kao, C. M.; Chen, C. T.; Nicholls, A. W.; Wu, X.; Shepherd, G. M. G.; Tian, B., Rational design of silicon structures for optically controlled multiscale biointerfaces. *Nat. Biomed. Eng.* **2018,** *2* (7), 508-521.
55. Rastogi, S. K.; Garg, R.; Scopelliti, M. G.; Pinto, B. I.; Hartung, J. E.; Kim, S.; Murphey, C. G. E.; Johnson, N.; San Roman, D.; Bezanilla, F.; Cahoon, J. F.; Gold, M. S.; Chamanzar, M.; Cohen-Karni, T., Remote nongenetic optical modulation of neuronal activity using fuzzy graphene. *Proc. Natl. Acad. Sci. USA* **2020,** *117* (24), 13339-13349.
56. Wang, Y.; Garg, R.; Hartung, J. E.; Goad, A.; Patel, D. A.; Vitale, F.; Gold, M. S.; Gogotsi, Y.; Cohen-Karni, T., Ti3C2Tx MXene Flakes for Optical Control of Neuronal Electrical Activity. *ACS Nano* **2021,** *15* (9), 14662-14671.
57. Yoo, S.; Hong, S.; Choi, Y.; Park, J. H.; Nam, Y., Photothermal inhibition of neural activity with near-infrared-sensitive nanotransducers. *ACS Nano* **2014,** *8* (8), 8040-8049.
58. Nachabe, R.; van der Hoorn, J. W.; van de Molengraaf, R.; Lamerichs, R.; Pikkemaat, J.; Sio, C. F.; Hendriks, B. H.; Sterenborg, H. J., Validation of interventional fiber optic spectroscopy with MR spectroscopy, MAS-NMR spectroscopy, high-performance thin-layer chromatography, and histopathology for accurate hepatic fat quantification. *Invest. Radiol.* **2012,** *47* (4), 209-216.
59. Jang, M.; Ruan, H.; Judkewitz, B.; Yang, C., Model for estimating the penetration depth limit of the time-reversed ultrasonically encoded optical focusing technique. *Opt. Express* **2014,** *22* (5), 5787-807.
60. Revision of guidelines on limits of exposure to laser radiation of wavelengths between 400 nm and 1.4 microm. International Commission on Non-Ionizing Radiation Protection. *Health Phys.* **2000,** *79* (4), 431-440.
61. Tsai, H. C.; Zhang, F.; Adamantidis, A.; Stuber, G. D.; Bonci, A.; de Lecea, L.; Deisseroth, K., Phasic firing in dopaminergic neurons is sufficient for behavioral conditioning. *Science* **2009,** *324* (5930), 1080-1084.

62. Magnus, C. J.; Lee, P. H.; Bonaventura, J.; Zemla, R.; Gomez, J. L.; Ramirez, M. H.; Hu, X.; Galvan, A.; Basu, J.; Michaelides, M.; Sternson, S. M., Ultrapotent chemogenetics for research and potential clinical applications. *Science* **2019,** *364* (6436).
63. Munshi, R.; Qadri, S. M.; Zhang, Q.; Castellanos Rubio, I.; Del Pino, P.; Pralle, A., Magnetothermal genetic deep brain stimulation of motor behaviors in awake, freely moving mice. *eLife* **2017,** *6*.
64. Alexander, G. M.; Rogan, S. C.; Abbas, A. I.; Armbruster, B. N.; Pei, Y.; Allen, J. A.; Nonneman, R. J.; Hartmann, J.; Moy, S. S.; Nicolelis, M. A.; McNamara, J. O.; Roth, B. L., Remote control of neuronal activity in transgenic mice expressing evolved G protein-coupled receptors. *Neuron* **2009,** *63* (1), 27-39.
65. Chen, R.; Romero, G.; Christiansen, M. G.; Mohr, A.; Anikeeva, P., Wireless magnetothermal deep brain stimulation. *Science* **2015,** *347* (6229), 1477-80.
66. Sebesta, C.; Torres Hinojosa, D.; Wang, B.; Asfouri, J.; Li, Z.; Duret, G.; Jiang, K.; Xiao, Z.; Zhang, L.; Zhang, Q.; Colvin, V. L.; Goetz, S. M.; Peterchev, A. V.; Dierick, H. A.; Bao, G.; Robinson, J. T., Subsecond multichannel magnetic control of select neural circuits in freely moving flies. *Nat. Mater.* **2022,** *21* (8), 951-958.
67. Grandl, J.; Kim, S. E.; Uzzell, V.; Bursulaya, B.; Petrus, M.; Bandell, M.; Patapoutian, A., Temperature-induced opening of TRPV1 ion channel is stabilized by the pore domain. *Nat. Neurosci.* **2010,** *13* (6), 708-14.
68. Luo, J.; Shen, W. L.; Montell, C., TRPA1 mediates sensation of the rate of temperature change in Drosophila larvae. *Nat. Neurosci.* **2017,** *20* (1), 34-41.
69. Moon, J.; Christiansen, M. G.; Rao, S.; Marcus, C.; Bono, D. C.; Rosenfeld, D.; Gregurec, D.; Varnavides, G.; Chiang, P. H.; Park, S.; Anikeeva, P., Magnetothermal Multiplexing for Selective Remote Control of Cell Signaling. *Adv. Funct. Mater.* **2020,** *30* (36), 2000577.
70. S. Link, M. B. M., and M. A. El-Sayed, Simulation of the Optical Absorption Spectra of Gold Nanorods as a Function of Their. *J. Phys. Chem. B* **1999,** *103* (16), 3073-3077.
71. Xiang, H. Y.; Lin, H. J.; Niu, T. T.; Chen, Z. Y.; Aigouy, L., Nanoscale thermal characterization of high aspect ratio gold nanorods for photothermal applications at $\lambda = 1.5$ μm. *J Appl Phys* **2019,** *125* (16), 163101.
72. Martino, N.; Kwok, S. J. J.; Liapis, A. C.; Forward, S.; Jang, H.; Kim, H. M.; Wu, S. J.; Wu, J.; Dannenberg, P. H.; Jang, S. J.; Lee, Y. H.; Yun, S. H., Wavelength-encoded laser particles for massively multiplexed cell tagging. *Nat. Photonics* **2019,** *13* (10), 720-727.
73. Zhang, Y.; Yang, D.; Nie, J.; Dai, J.; Wu, H.; Zheng, J. C.; Zhang, F.; Fang, Y., Transcranial Non-genetic Neuromodulation Via Bioinspired Vesicle-Enabled Precise NIR-II Optical-stimulation. *Adv. Mater.* **2022**, e2208601.
74. Jiang, Y.; Lee, H. J.; Lan, L.; Tseng, H. A.; Yang, C.; Man, H. Y.; Han, X.; Cheng, J. X., Optoacoustic brain stimulation at submillimeter spatial precision. *Nat. Commun.* **2020,** *11*, 881.
75. Jiang, Y.; Huang, Y. M.; Luo, X. Y.; Wu, J. Y. Z.; Zong, H. N.; Shi, L. L.; Cheng, R.; Zhu, Y. F.; Jiang, S.; Lan, L.; Jia, X. T.; Mei, J. G.; Man, H. Y.; Cheng, J. X.; Yang, C., Neural Stimulation In Vitro and In Vivo by Photoacoustic Nanotransducers. *Matter* **2021,** *4* (2), 645-674.
76. Parameswaran, R.; Carvalho-de-Souza, J. L.; Jiang, Y.; Burke, M. J.; Zimmerman, J. F.; Koehler, K.; Phillips, A. W.; Yi, J.; Adams, E. J.; Bezanilla, F.; Tian, B., Photoelectrochemical modulation of neuronal activity with free-standing coaxial silicon nanowires. *Nat. Nanotechnol.* **2018,** *13* (3), 260-266.
77. Maya-Vetencourt, J. F.; Manfredi, G.; Mete, M.; Colombo, E.; Bramini, M.; Di Marco, S.; Shmal, D.; Mantero, G.; Dipalo, M.; Rocchi, A.; DiFrancesco, M. L.; Papaleo, E. D.; Russo, A.;

Barsotti, J.; Eleftheriou, C.; Di Maria, F.; Cossu, V.; Piazza, F.; Emionite, L.; Ticconi, F.; Marini, C.; Sambuceti, G.; Pertile, G.; Lanzani, G.; Benfenati, F., Subretinally injected semiconducting polymer nanoparticles rescue vision in a rat model of retinal dystrophy. *Nat. Nanotechnol.* **2020,** *15* (8), 698-708.
78. DiFrancesco, M. L.; Lodola, F.; Colombo, E.; Maragliano, L.; Bramini, M.; Paterno, G. M.; Baldelli, P.; Serra, M. D.; Lunelli, L.; Marchioretto, M.; Grasselli, G.; Cimo, S.; Colella, L.; Fazzi, D.; Ortica, F.; Vurro, V.; Eleftheriou, C. G.; Shmal, D.; Maya-Vetencourt, J. F.; Bertarelli, C.; Lanzani, G.; Benfenati, F., Neuronal firing modulation by a membrane-targeted photoswitch. *Nat. Nanotechnol.* **2020,** *15* (4), 296-306.
79. Prominski, A.; Shi, J.; Li, P.; Yue, J.; Lin, Y.; Park, J.; Tian, B.; Rotenberg, M. Y., Porosity-based heterojunctions enable leadless optoelectronic modulation of tissues. *Nat. Mater.* **2022,** *21* (6), 647-655.
80. Chen, K. T.; Wei, K. C.; Liu, H. L., Theranostic Strategy of Focused Ultrasound Induced Blood-Brain Barrier Opening for CNS Disease Treatment. *Front. Pharmacol.* **2019,** *10*, 86.
81. Szablowski, J. O.; Lee-Gosselin, A.; Lue, B.; Malounda, D.; Shapiro, M. G., Acoustically targeted chemogenetics for the non-invasive control of neural circuits. *Nat. Biomed. Eng.* **2018,** *2* (7), 475-484.
82. Sirsi, S. R.; Borden, M. A., State-of-the-art materials for ultrasound-triggered drug delivery. *Adv. Drug. Deliv. Rev.* **2014,** *72*, 3-14.
83. Chen, X.; Chen, Y.; Xin, H.; Wan, T.; Ping, Y., Near-infrared optogenetic engineering of photothermal nanoCRISPR for programmable genome editing. *Proc. Natl. Acad. Sci. USA* **2020,** *117* (5), 2395-2405.
84. Miller, I. C.; Zamat, A.; Sun, L. K.; Phuengkham, H.; Harris, A. M.; Gamboa, L.; Yang, J.; Murad, J. P.; Priceman, S. J.; Kwong, G. A., Enhanced intratumoural activity of CAR T cells engineered to produce immunomodulators under photothermal control. *Nat. Biomed. Eng.* **2021,** *5* (11), 1348-1359.
85. Rommelfanger, N. J.; Brinson, K., Jr.; Bailey, J. E.; Bancroft, A. M.; Ou, Z.; Hong, G., Pristine carbon nanotubes are efficient absorbers at radio frequencies. *Nanotechnology* **2022,** *33* (34), 345102.
86. Rommelfanger, N. J.; Hong, G., On the feasibility of wireless radio frequency ablation using nanowire antennas. *APL Mater.* **2021,** *9* (7), 071103.
87. Rommelfanger, N. J.; Ou, Z.; Keck, C. H. C.; Hong, G., Differential heating of metal nanostructures at radio frequencies. *Phys. Rev. Appl.* **2021,** *15* (5), 054007.

Figures

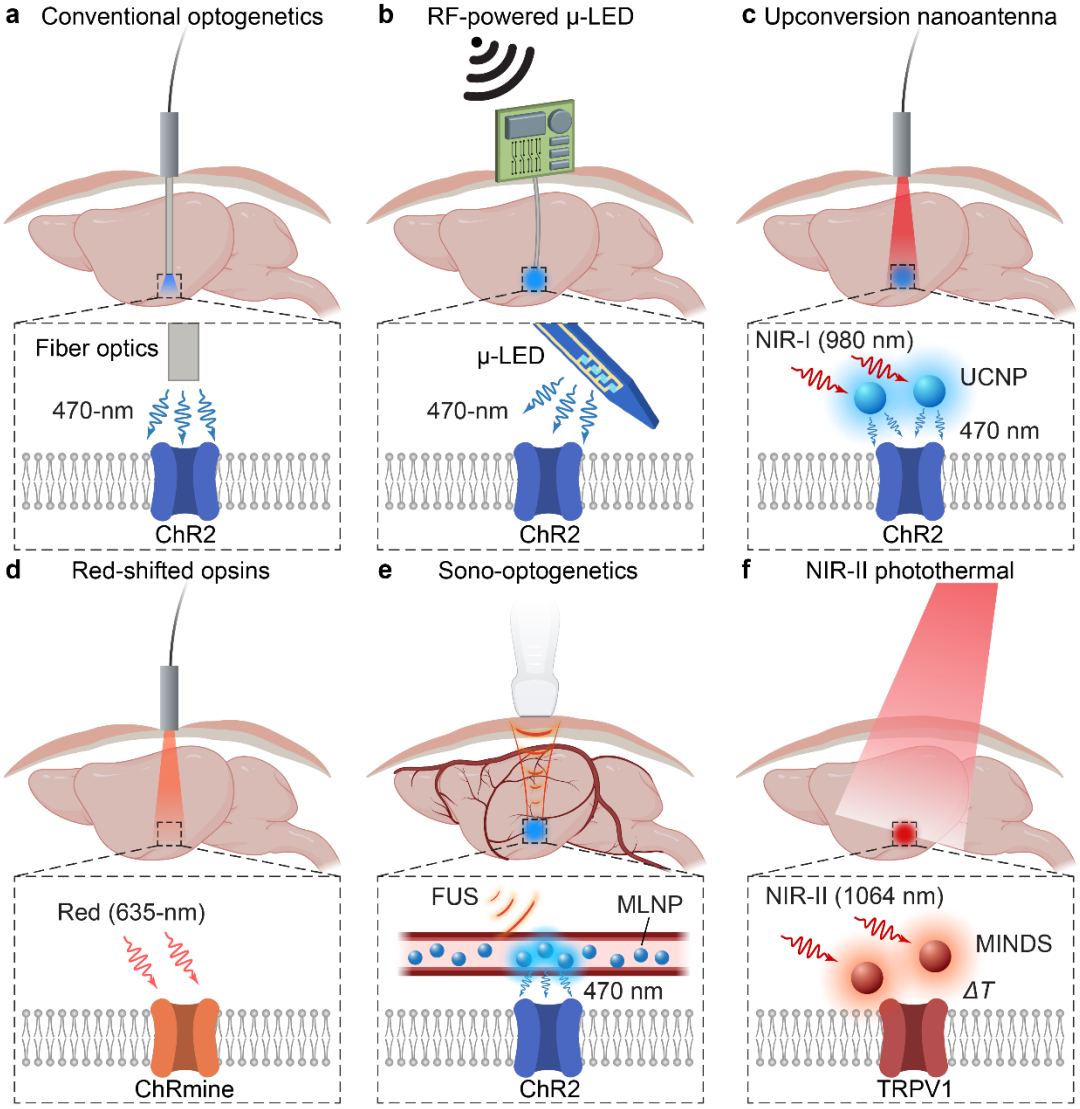

Figure 1. Optical methods for deep-brain neuromodulation. (**a**) Conventional optogenetics with an implanted optical fiber.[8] (**b**) Wireless optogenetics based on RF-powered μ-LED devices.[13, 32-34] (**c**) Transcranial optogenetics based on upconversion nanoantennas and NIR-I illumination.[14] (**d**) Transcranial optogenetics based on the red-shifted opsin, ChRmine.[12] (**e**) Sono-optogenetics based on transcranial FUS and circulation-delivered MLNPs.[15, 42, 45] (**f**) Tether-free NIR-II photothermal neuromodulation based on MINDS and TRPV1. Adapted with permission from Ref. 22.

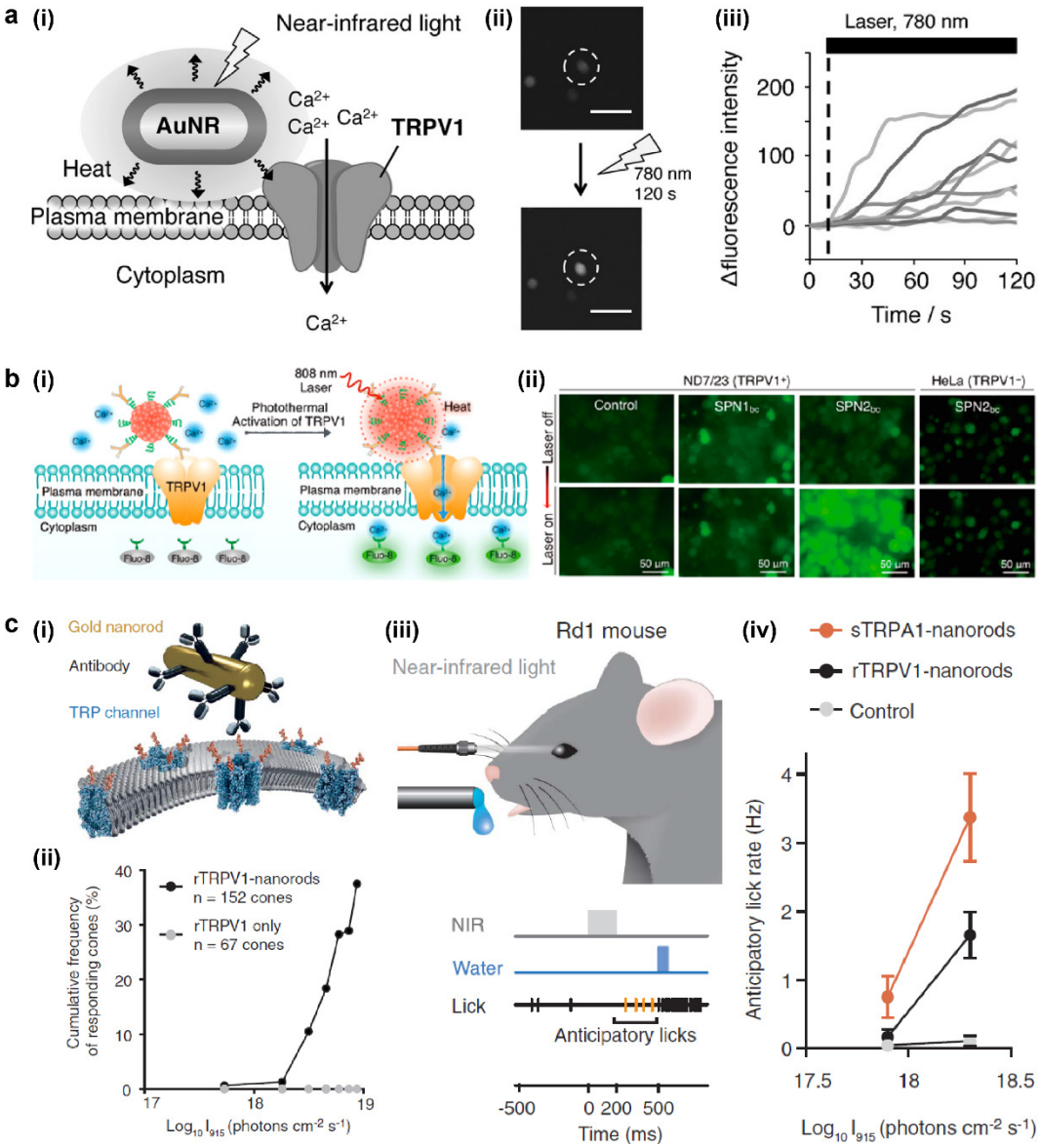

Figure 2. Photothermal neuromodulation via TRP channel activation. (**a**) (i) Schematics of photothermal activation of TRPV1-expressing HEK293T cells with AuNRs and NIR light. (ii) Fluorescence images of cells before (top) and after (bottom) NIR illumination. The scale bars represent 100 μm. (iii) Calcium-dependent fluorescence intensity dynamics upon NIR illumination. Adapted with permission from Ref. 19. Copyright 2015, Wiley-VCH. (**b**) (i) Schematics of photothermal stimulation of TRPV1-expressing cells with SPN and NIR light. (ii) Fluorescence images of ND7/23 (TRPV1+) and HeLa (TRPV1-) cells under different experimental conditions. Adapted with permission from Ref. 51. Copyright 2016, American Chemical Society. (**c**) (i) Schematics of TRP channel activation in the retina via AuNRs and NIR light. (ii) Cumulative frequency of responding TRPV1-expressing cones with and without AuNRs upon NIR illumination. (iii) Schematics of behavioral tasks during photothermal stimulation of the mouse retina. (iv) Anticipatory lick rate as a function of NIR intensity for mice with sTRPA1, or rTRPV1, or neither. Adapted with permission from Ref. 52. Copyright 2020, American Association for the Advancement of Science.

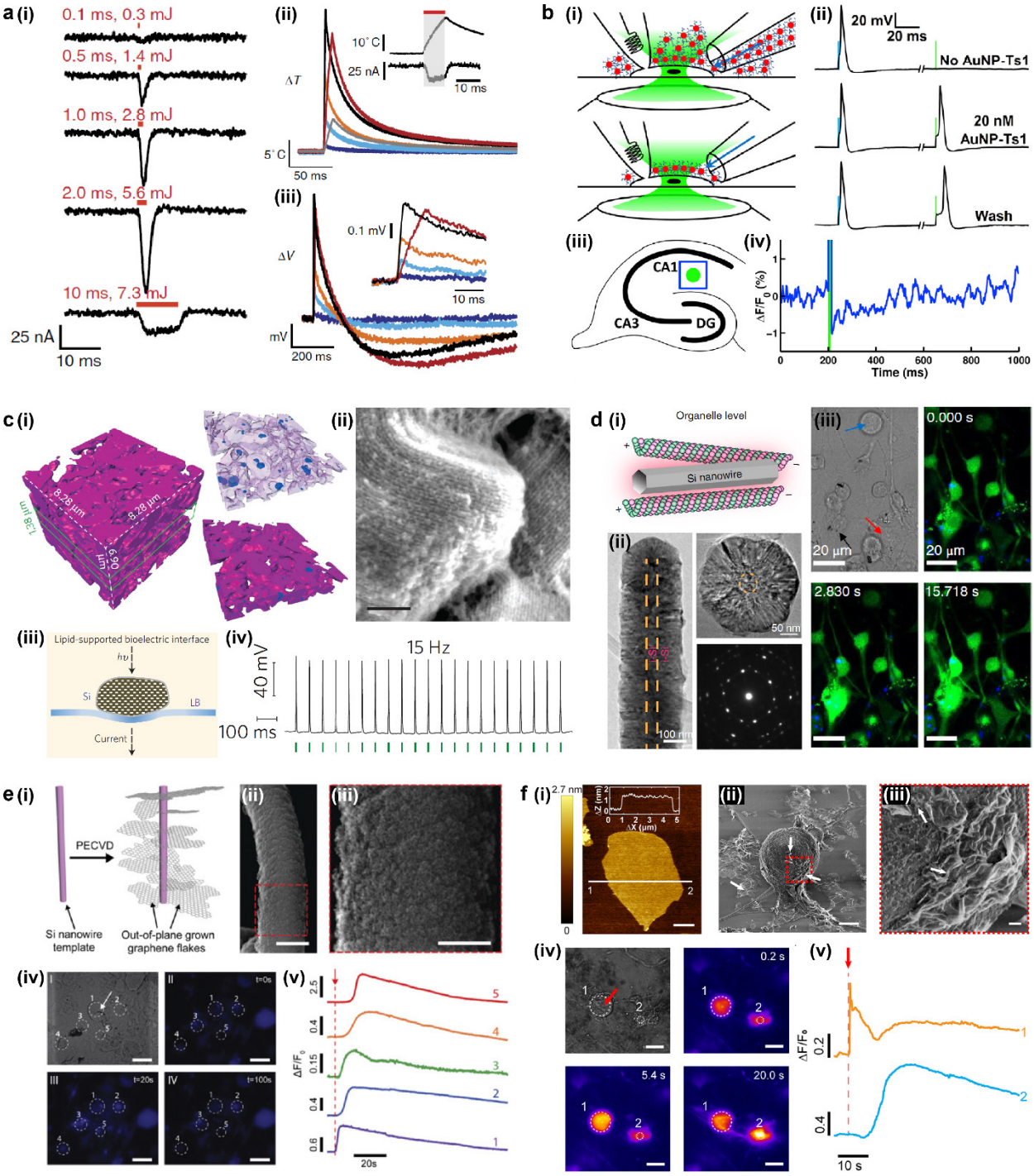

Figure 3. Photothermal neuromodulation via membrane capacitance change. (**a**) (i) Current measurement of voltage-clamped oocytes under the stimulation of NIR light pulses (red lines). (ii, iii) Local temperature (ii) and voltage (iii) measurements of oocytes membrane under NIR light pulses, showing the mechanism of photothermal neuromodulation via membrane capacitance change. Adapted with permission from Ref. 20. Copyright 2012, Nature Publishing Group. (**b**) (i) Schematics showing the perfusion of surface-functionalized AuNPs, which adhere to the cell membrane even after washing. (ii) Current measurement from DRG neurons under green light

stimulation with or without AuNPs. (iii) Schematics of photothermal stimulation of mouse hippocampal slices via AuNPs and green light. (iv) Fluorescence intensity of voltage-sensitive dye in the mouse hippocampal slice upon green light stimulation. Adapted with permission from Ref. 53. Copyright 2015, Elsevier Inc.. (**c**) (i, ii) Reconstructed X-ray microscopy 3D structure (i) and SEM image (ii) of mesostructured silicon. (iii) Schematic of photothermal stimulation with mesostructured silicon. (iv) Voltage measurement of DRG neurons under 15 Hz green light stimulation. Adapted with permission from Ref. 18. Copyright 2016, Nature Publishing Group. (**d**) (i) Schematics of silicon nanowire interfacing with intracellular organelles. (ii) TEM image and SAED pattern of a silicon nanowire. (iii) Brightfield and fluorescence images of neurons and glia cells after green light stimulation. Adapted with permission from Ref. 54. Copyright 2018, Nature Publishing Group. (**e**) (i) Schematics showing the production of 3D graphene flakes. (ii, iii) SEM images of 3D graphene flakes. Scale bars represent 1 μm in (ii) and 500 nm in (iii). (iv, v) Brightfield and fluorescence images (iv), and temporal dynamics of fluorescence intensity (v) of DRG neurons upon red light stimulation. Adapted with permission from Ref. 55. Copyright 2020, National Academy of Sciences. (**f**) (i) AFM image of a single-layer $Ti_3C_2T_x$ flake. (ii, iii) SEM images of $Ti_3C_2T_x$ flakes interfacing with a DRG neuron. Scale bars represent 10 μm in (ii) and 1 μm in (iii). (iv, v) Brightfield and fluorescence images (iv), and temporal dynamics of fluorescence intensity (v) of DRG neurons upon red light stimulation. Adapted with permission from Ref. 56. Copyright 2021, American Chemical Society.

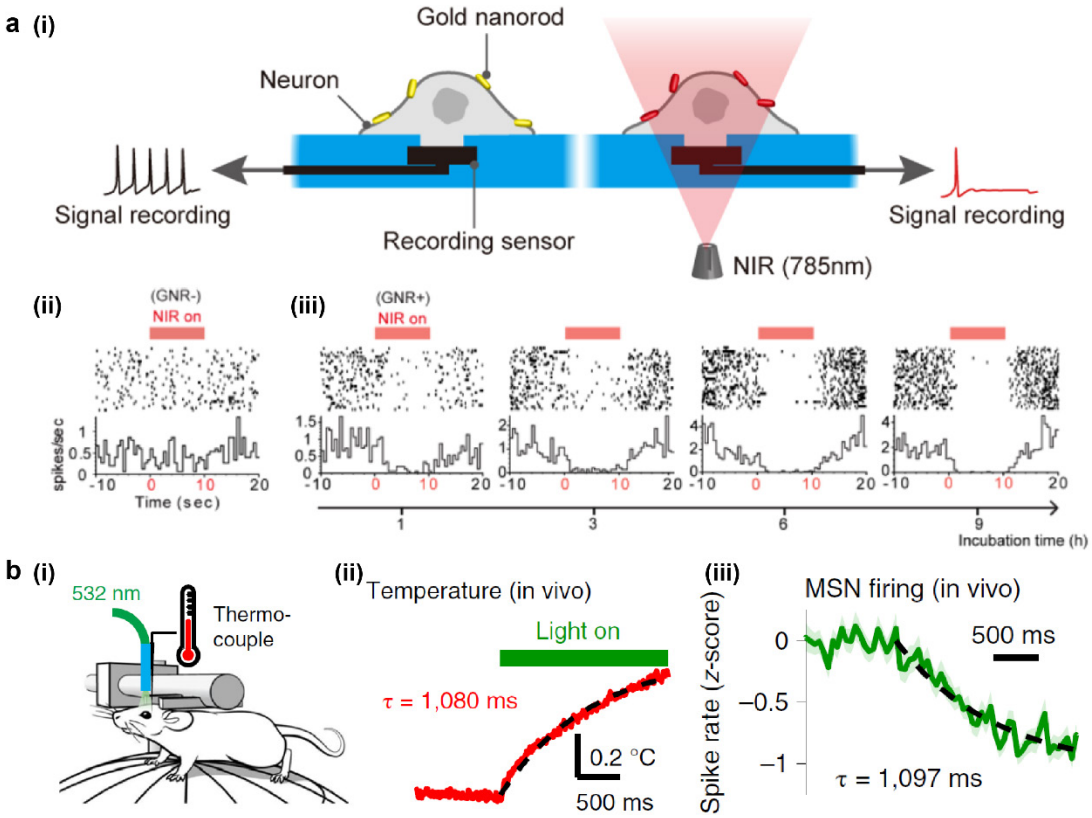

Figure 4. Photothermal inhibition of neural activities. (**a**) (i) Schematics of photothermal inhibition of neural activities with AuNRs and NIR light. (ii, iii) Neural firing rates upon NIR illumination before (ii) and after (iii) incubation with AuNRs. Adapted with permission from Ref. 57. Copyright 2014, American Chemical Society (**b**) (i) Schematics for the experiment setup of spontaneous measurement of temperature and electrophysiology *in vivo* during green light stimulation. (ii, iii) Temperature (ii) and neural firing rate dynamics (iii) in mouse MSNs upon green light stimulation. Adapted with permission from Ref. 38. Copyright 2019, Nature Publishing Group.

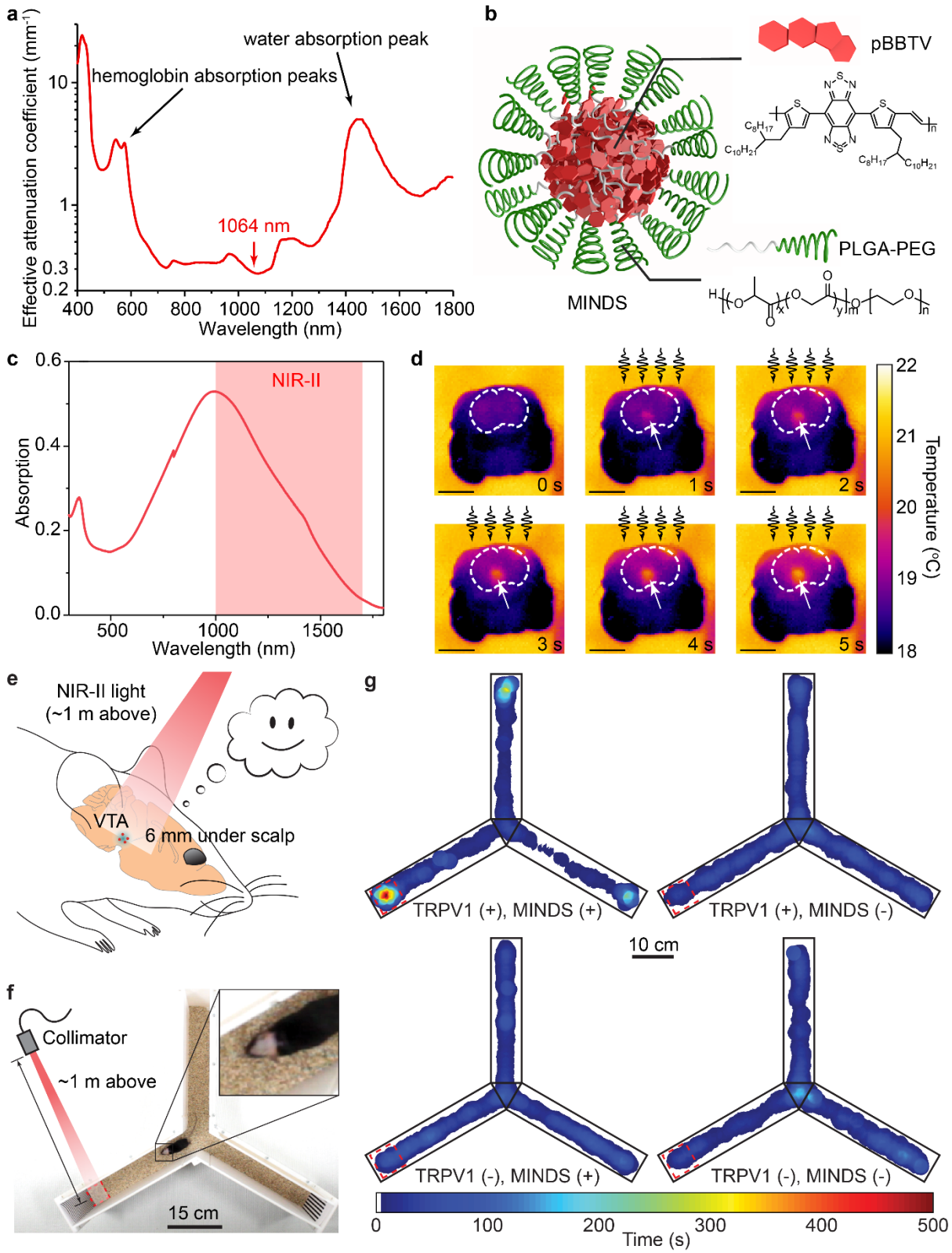

Figure 5. NIR photothermal neuromodulation with MINDS. (**a**) The effective attenuation coefficient of brain tissue in the 400-1800 nm spectrum. (**b**) Schematic showing the design of

MINDS. (**c**) Absorption spectrum of MINDS. (**d**) Cross-sectional thermal images of a mouse head at different time points after through-scalp wide-field 1064-nm illumination. The white arrows highlight the MINDS injection site. The scale bars represent 5 mm. (**e**) Schematics showing NIR-II neuromodulation of reward circuitry in the mouse brain. (**f**) A photo showing the setup of the conditioned place preference test inside a Y-maze. (**g**) Post-test heat maps showing the time of travel of mice with different experimental conditions. Adapted with permission from Ref. 22.

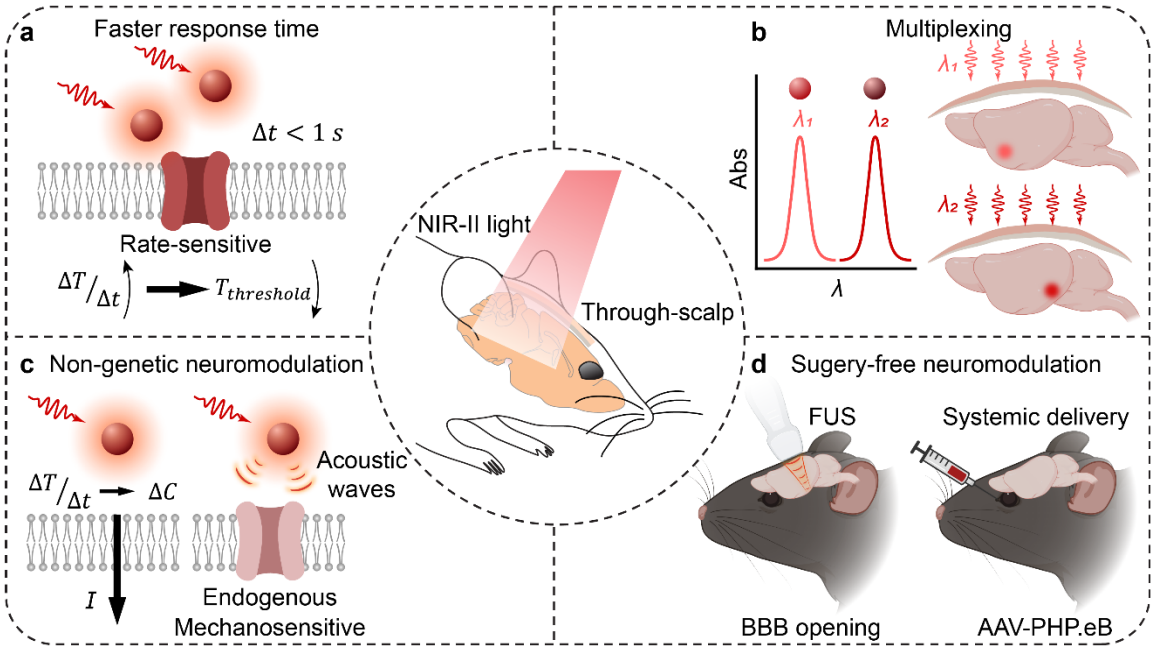

Figure 6. Future directions for NIR-II deep-brain neuromodulation methods. (**a**) A faster response time can be achieved with temperature-rate sensitive ion channels.[66] (**b**) Multichannel stimulation can be achieved via photothermal systems with sharp and non-overlapping absorption peaks.[66, 69-71] (**c**) Non-genetic NIR-II deep-brain neuromodulation may be achieved with highly absorbing and efficient photothermal nanotransducers via either the membrane capacitance change or the acoustic activation mechanism.[73-75] (**d**) Surgery-free NIR-II deep-brain neuromodulation can be achieved with systemic delivery of transgenes and MINDS, either via ultrasound-mediated BBB opening or engineered AAVs with brain tropism.[41, 80, 81] Adapted with Permission from Ref. 22.